Chemical Geology 690 (2025) 122884

Contents lists available at ScienceDirect

Chemical Geology

journal homepage: www.elsevier.com/locate/chemgeo

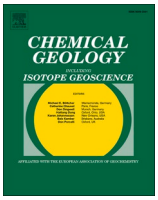

Research Paper

The influence of primary depositional conditions on Hg behaviour during early thermal maturation

Asri O. Indraswari [a,b,*], Joost Frieling [a], Erdem Idiz [a], Tamsin A. Mather [a], Alexander J. Dickson [c], Hugh C. Jenkyns [a], Stuart A. Robinson [a], Isabel M. Fendley [a,d], Oliver Neilson [d]

[a] Department of Earth Sciences, University of Oxford, South Parks Road, Oxford OX1 3AN, UK
[b] Department of Geosciences, Faculty of Mathematics and Natural Sciences (FMIPA), Universitas Indonesia, Depok 16424, Indonesia
[c] Centre of Climate, Ocean and Atmosphere, Department of Earth Sciences, Royal Holloway University of London, Egham, Surrey TW20 0EX, UK
[d] Department of Geosciences, Pennsylvania State University, University Park, PA, USA

ARTICLE INFO

Editor: Claudia Romano

Dataset link: Data for: The influence of primary depositional conditions on Hg behaviour during early thermal maturation (Original data)

Keywords:
Mercury
Hg
Thermal maturation
Volatilization
Organic matter
Belemnite Marls
Tanjung Formation
Posidonienschiefer
Pyrolysis
Primary deposition

ABSTRACT

Mercury (Hg) behaviour in sedimentary rocks is important to understand both in terms of its potential volatilization during magmatic intrusions (e.g., those associated with large igneous province activity) and its redistribution during thermal maturation associated with burial and, in some cases, hydrocarbon generation. Mercury behaviour varies significantly across different lithologies, likely influenced by the amount and type of organic matter present and sulfur chemistry. This study investigates the effects of lithology on Hg dynamics during thermal maturation through pyrolysis experiments at isothermal conditions of 325 °C for various durations (24, 336, 500, and 840 h). To study Hg behaviour in different lithologies, representing different depositional environments and OM-types (organic-rich vs organic-lean), we analysed a relatively Hg-rich sample from the Lower Jurassic (Pliensbachian) Belemnite Marls, a marine carbonate-rich sequence exposed in southern England, and a coal sample from the Eocene Tanjung Formation, Indonesia composed of terrestrial organic matter. Before and after pyrolysis, we generated data on Hg concentrations, total organic carbon (TOC), hydrogen index (HI), and oxygen index (OI) and compared our results with existing data from the Posidonienschiefer, a marine, highly organic-rich, black shale of Toarcian age from Germany. Results indicate substantial Hg loss, with the coal and Belemnite Marls samples losing over 80 % of their Hg in the first 24 h, compared to a 50 % loss in the Posidonienschiefer. Thermal desorption profiles (TDPs) allow us to align the Hg losses in the isothermal heating experiments with the initial Hg speciation in the sedimentary rocks. Both the Belemnite Marls sample and Tanjung Formation coal are dominated by lower temperature Hg species, potentially bound to or associated with organic matter. These findings enhance our understanding of the interplay between lithology, thermal maturation, and Hg behaviour, which is critical for interpreting historical Hg cycling and the environmental impacts associated with the formation of large igneous provinces (LIPs).

1. Introduction

Mercury (Hg) anomalies in the sedimentary record are increasingly recognized as a valuable proxy for studying large igneous provinces (LIPs) and their environmental impacts (Sanei et al., 2012; Grasby et al., 2019; Percival et al., 2021). While this proxy has been mostly used as a qualitative metric of LIP activity, under the right circumstances it might be possible to use Hg to estimate carbon emissions during carbon-cycle perturbation events based on Hg sedimentary contents, mercury cycle models, and realistic Hg/C emission ratios (Fendley et al., 2024). A proportion of both carbon and Hg emissions associated with LIPs is potentially sourced from thermogenic release from intruded sediments as well as the magmatic volatile load (Ganino and Arndt, 2009). This proportion depends on the scale of the intrusions and the nature of the intruded rocks. Specifically, the intruded rocks may vary not only in both organic-matter and Hg content but also in their potential to generate fluids and gases, and their potential for Hg release may depend on its speciation as well as the feasibility of the fluids generated escaping to the surface. There is growing interest in understanding how Hg and C behave near intrusives within LIPs (Svensen et al., 2023a; Frieling et al.,

* Corresponding author at: Department of Geosciences, Faculty of Mathematics and Natural Sciences (FMIPA), Universitas Indonesia, Depok 16424, Indonesia
E-mail address: asrioktavioni@ui.ac.id (A.O. Indraswari).

https://doi.org/10.1016/j.chemgeo.2025.122884
Received 5 March 2025; Received in revised form 14 May 2025; Accepted 24 May 2025
Available online 26 May 2025

2025): a comprehensive overview of Hg and organic-matter behaviour with thermal maturation can be used to inform how intrusions into specific rock-types or under particular environmental conditions may influence Hg/C of thermogenic gases and refine Hg-based LIP emissions.

The volatiles produced and released along with Hg by these intrusives can range from hydrocarbon gases and CO_2, to larger molecular-weight hydrocarbons (Svensen et al., 2023b and references therein), influenced by the temperature (i.e., distance from the intrusion) and the bulk compositions of the intruded rocks. Close to the igneous intrusion, the sediments may be exposed to very high temperatures and, with increasing exposure temperature, the resulting products will gradually become more enriched in dry gases (CH_4 and CO_2) as a result of cracking of the sedimentary organic matter and generated heavier hydrocarbons (Goodarzi et al., 2018). Furthermore, the behaviour of Hg during subsidence-related (burial) thermal maturation has also gained attention, with a focus on understanding Hg in generated and mobilized fluids (e.g., Bryndzia et al., 2023; Indraswari et al., 2024).

Mercury can be hosted in various sedimentary phases, for example, organic matter (OM) and metal sulfides (e.g., pyrite, (meta-)cinnabar HgS) (Grasby et al., 2019; Shen et al., 2019). Whether influenced by magmatic intrusions or basin subsidence, sedimentary OM and other components (i.e., water, clays) undergo transformation (thermal maturation) in response to elevated temperature and pressure, which can result in, for example, the redistribution of carbon and Hg between solid and fluid phases (both hydrocarbon and non-hydrocarbon). The generated fluids provide a potential pathway for mobilizing and facilitating Hg transport between geological rock reservoirs and the surface. Although metals are often assumed to be closely associated with OM, previous studies have observed only minor partitioning of elements such as Mo, Zn, U, and Cd into the hydrocarbon fluids during maturation (Dickson et al., 2020, 2022; Kendall et al., 2023). We have recently found evidence via isothermal pyrolysis experiments that the same situation applies to Hg (Indraswari et al., submitted), which showed only very limited ($\leq$ 1 %) partitioning into a hydrocarbon phase during maturation, at least for a highly organic-rich marine black shale.

The type and concentration of organic matter (OM) in sediments strongly influences the quantity and composition of fluids generated and expelled during thermal maturation (Tissot and Welte, 1984). This principle may also extend to the behaviour of sediment-hosted mercury (Hg). Recent studies, including artificial maturation experiments and investigations of sedimentary rocks affected by igneous intrusions, have explored the isotopic variations of Hg under thermal maturation (e.g., Liu et al., 2022; Chen et al., 2022). However, these studies have not focused on the depositional environments of the samples that may have had an influence on Hg behaviour during maturation through differences in both OM type and concentration as well as Hg speciation. Consequently, the influence of varying depositional environments on sedimentary Hg behaviour during thermal maturation remains poorly understood. This knowledge gap is particularly important when considering the heterogeneous nature of sediments exposed to LIP-related metamorphism. This study aims to contribute to addressing this gap by examining how different depositional settings affect the thermal behaviour of Hg in sedimentary rocks.

Table 1 outlines the different depositional settings of samples previous researchers have used when looking at the effect of thermal maturation, both burial- and intrusion-related, on Hg. The sediments in question consist mainly of marine black shales (Liu et al., 2022; Chen et al., 2022; Svensen et al., 2023a; Frieling et al., 2025), but also lacustrine shales and calcareous mudstones (Liu et al., 2022), as well as a recent soil (Chen et al., 2022) (Table 1). These studies all showed significant Hg loss due to the high potential for sedimentary Hg species to decompose, especially in a temperature range of 200–300 °C (Chen et al., 2022; Liu et al., 2022; Svensen et al., 2023a; Frieling et al., 2025). However, between different sample types, we find there are significant differences in Hg behaviour (Fig. 1). This result is not unexpected as different sediment types and depositional settings will likely cover a range of variations in OM types, and organic and inorganic S-containing

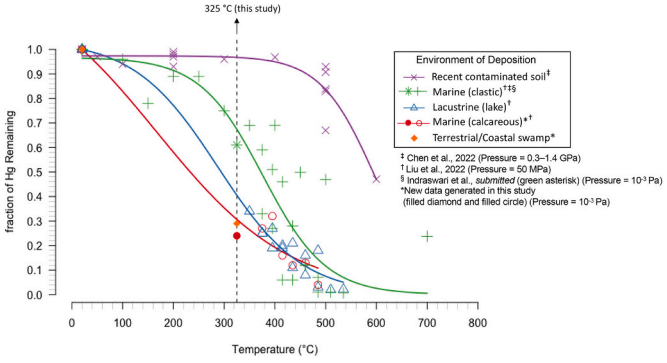

Fig. 1. Mercury fraction remaining relative to the original concentration in different materials in response to artificial heating of less than 25 h (previous studies used heating durations of $\leq$25 h). Fitted lines are sigmoidal curves to represent cumulative Hg loss. Fraction of Hg remaining = $(1 / (1+ b \times e^{cx}))$, where x is peak exposure temperature, b and c are fitted constants.

Table 1
Summary of the depositional environments, redox conditions, and lithologies used in experimental studies examining the effects of thermal maturation, both burial- and intrusion-related, on sedimentary Hg.

Age	Formation /Member Name	Environment of deposition	Oxygenation regime	Potential for sulfide production	Kerogen Type	Lithology	Initial bulk TOC (%)	Initial Total Hg (ppb)	Reference
Mesoprotero-zoic	Xiamaling Formation	Marine	Suboxic	Moderate to high	Oil-prone (II)	Black shale	4.09 13.35	326.8 107.3	Liu et al., 2022
Permian	Talung Formation	Marine	Suboxic-anoxic	Moderate	Oil-prone (II)	Calcareous mudstone	5.56	238.7	
Eocene	Shahejie Formation	Lacustrine	Anoxic	Moderate to high	Oil-prone (I/II)	Black shale	3.45 4.83	272.4 178.1	
Proterozoic (Cryogenian)	Datangpo Formation	Marine	Anoxic	High	Oil-prone (I/II)	Black shale	1.91	375	Chen et al., 2022
Recent	–	Limestone-weathered soil	Unknown	Unknown, likely low	Unknown	Contaminated soil	0.62	563	
Lower Jurassic	Posidonienschiefer	Marine	Euxinic	High	Oil-prone (II)	Black shale	8.85	74.6	Indraswari et al., submitted
Lower Jurassic	Belemnite Marls	Marine	Dysoxic	Moderate	Inert (IV)	Calcareous mudstone	0.85	325.4	**This study**
Eocene	Tanjung Formation	Terrestrial/ Coastal swamps	Dysoxic	Low but non-zero	Oil and gas-prone (II/III)	Coal	24.73	44.2	

species (sulfides, sulfates, thiols) and Hg compounds defined based on sequential extraction and thermal mercury release characteristics (OM-bound, pyrite-bound, (meta-)cinnabar) – all factors that we hypothesize play an important role in the sequestration, release and mobilization of Hg in response to thermal maturation.

It is also worth noting that in the majority of existing studies using Hg signals as LIP, the most prominent Hg signals are often found in TOC-lean lithologies rather than in organic-rich shales (see e.g., Grasby et al., 2019). This observation further motivates our multi-lithology approach in the present study, which aims to expand the mechanistic understanding of Hg mobility beyond typical black shale contexts and to improve the interpretation of Hg signals across a wider range of depositional environments.

In order to address the role of the depositional environment and organic-matter variability on Hg behaviour during thermal maturation, and to complement a previous study carried out on a Jurassic marine organic-rich marly sediment (Posidonienschiefer) with Type II kerogen (Indraswari et al., submitted), we performed pyrolysis experiments on two additional types of samples. We selected a carbonate-rich organic-lean marl sample from the Lower Jurassic Belemnite Marls sequence that has atypically elevated Hg contents (>300 ppb). The organic matter is Type IV kerogen (non-source rock) and the sediment was deposited in a shallow-marine epicontinental basin. Although the Belemnite Marls sequence has significant variability in both TOC content and quality (Lang et al., 1928; Weedon and Jenkyns, 1990, 1999; Hesselbo and Jenkyns, 1995), the organic-lean and Hg enriched material we selected provides an end-member so far unrepresented in maturation experiments (Fig. 1). The second sample, from the Eocene Tanjung Formation, is a terrestrial coal deposited in a tidally influenced lower coastal plain (Type II/III Kerogen) with moderate Hg but high organic carbon. As in our previous study (Indraswari et al., submitted), we conducted artificial maturation experiments under isothermal conditions at 325 °C for 24, 168, 336, 500, and 840 h. These new datasets were compared with existing pyrolysis data from the Posidonienschiefer (Indraswari et al., submitted) and published data on Hg in artificially and naturally matured marine shales, lacustrine shales and marine carbonate-rich mudstones (Liu et al., 2022; Chen et al., 2022; Frieling et al., 2025).

The heating temperature used in the experiments is particularly significant, as the primary range for Hg loss, between 200 and 300 °C, is also where the greatest variability in Hg behaviour has been observed during pyrolysis analysis (see e.g., Fig. 1 and Frieling et al., 2025). While these temperatures are lower than the magmatic temperatures of intrusions, they are highly relevant to the thermal conditions experienced by surrounding sedimentary rocks during contact metamorphism, where temperatures of ~200–300 °C are commonly reached in distal aureole zones (e.g., Svensen et al., 2004, 2007). To build on previous studies that typically used shorter durations of around 24 h, we conducted longer term isothermal analyses. These extended experiments provide valuable insights into how Hg loss progresses under stable temperature conditions, a closer (albeit still limited) representation of situations that occur near igneous intrusions or in deeply buried sediments. While our experiments are not intended to directly replicate LIP-related contact metamorphism, they provide important constraints on how lithological variability may control Hg release potential. These insights are broadly relevant not only for refining models of Hg emissions during LIP events, but also for understanding Hg cycling during sediment burial and diagenesis more generally. We specifically focus on how different environmental conditions during deposition may have influenced sedimentary Hg behaviour during thermal maturation by examining the differences in redox state, availability of sulfur (which affects the presence of specific sulfide minerals) and organic-matter type. In contrast to earlier work, our study systematically compares three distinct sediment types (i.e., marine calcareous, marine euxinic, and terrestrial coal) to directly assess how variations in initial Hg speciation, shaped by depositional redox conditions and organic matter type, influence Hg release during thermal maturation. This comparison across different lithologies provides novel insights that extend beyond the commonly studied organic-rich marine shales, offering broader implications for understanding Hg cycling across various depositional settings.

2. Materials & methods

2.1. Sample material

We conducted maturation experiments for two new samples (organic-lean Belemnite Marls sample and organic-rich Tanjung Formation coal) and compare these to material used in previous studies looking at the effect of thermal maturation on Hg (Table 1). Comparative material includes the marine mudrocks of the Lower Jurassic Posidonienschiefer (Indraswari et al., submitted), the Proterozoic Xiamaling Formation, the Permian Talung Formation (Liu et al., 2022), Cryogenian Datangpo Formation (Chen et al., 2022), lacustrine shales from the Eocene Shahejie Formation (Liu et al., 2022), and highly contaminated recent GSS-4 soil standard reference material (Chen et al., 2022) (Table 1).

2.1.1. Depositional setting of the Belemnite Marls

The Belemnite Marls comprise a cyclically bedded alternation of light and dark marls and rare concretionary limestones packaged in decimetre-scale couplets and metre-scale bundles. The sequence is of Pliensbachian (Early Jurassic) age and was deposited in the Wessex Basin of southern England. The samples were collected from outcrops on the Dorset coast (Lang et al., 1928; Weedon and Jenkyns, 1990, 1999). Key sedimentary components are varying amounts of calcium carbonate, partially coccolith-derived, clay minerals (dominantly illite), organic matter and pyrite. The sequence is rich in body fossils such as belemnites, ammonites, bivalves, brachiopods and crinoids, signifying that the depositional environment was fully marine (Sellwood, 1970, 1972). The presence of *Chondrites* burrows throughout the section, signals relatively low oxygen (dysoxic) conditions (Bromley and Ekdale, 1984; Buatois and Mángano, 2016; Baucon et al., 2020). The burrowing mixed light-coloured sediment into dark and vice versa, and together with the local presence of black laminated shale in the succession, indicates the primary nature of the sedimentary cyclicity, attributed to astronomical (Milankovitch) forcing (Weedon and Jenkyns, 1990, 1999).

The specific sample used in this study is from sample BM-15, taken from the 15.09 m level in the section (Top 113c Bed) according to the numbering system of Lang et al. (1928) and stratigraphic log of Weedon and Jenkyns (1999). This specific layer is a light marl that is carbonate-rich and relatively poor in organic matter, with TOC of 0.85 % and $CaCO_3$ of 52.72 %. In general, the light marls in the sequence have mean TOC of 0.94 % and $CaCO_3$ of 58.8 % (Weedon and Jenkyns, 1990).

2.1.2. Depositional setting of the Tanjung Formation

The Tanjung Formation, deposited in the Barito Basin during the Middle Eocene to Early Oligocene in the Sundaland margin, is characterized by thick, laterally extensive planar coals formed in fluvial-tidal and marginal marine environments (Witts et al., 2012; Anggara et al., 2024). The coals in the Tanjung Formation contain mixed fresh- and brackish-water palynomorph assemblages and were interpreted as estuarine (non-deltaic) coastal swamp deposits due to their lateral continuity and stability (Witts et al., 2012). The coal is mainly composed of huminite macerals, with significant amounts of cutinite and resinite, along with inorganic constituents such as clay (kaolinite), pyrite, and carbonate minerals (Fikri et al., 2022; Anggara et al., 2024). The specific sample used in this study is from sample BT 110 from Witts et al. (2012) containing TOC of 24.73 % and has vitrinite reflectance of 0.37 %. Anggara et al. (2024) performed proximate and ultimate analyses of Tanjung Formation coals (n = 35). The proximate analysis, which measures moisture, fixed carbon, volatile matter, and ash content, revealed an average volatile matter of 44.6 %, fixed carbon of 40.1 %,

and low moisture content (4.2 %). The ultimate analysis, which determines the chemical composition of coal (i.e., percentages of carbon, hydrogen, nitrogen, oxygen, and sulphur) on a moisture- and volatile matter-free basis, showed high carbon (80 %), hydrogen (6.3 %), nitrogen (1.5 %), and total sulfur (1.6 %) contents. Vitrinite reflectance of 0.52–0.59 % Ro (Fikri et al., 2022), indicated that the coals are at the subbituminous A or high volatile bituminous C stage, and immature with respect to hydrocarbon generation (Tissot and Welte, 1984). Patria et al. (2024) observed that framboidal pyrite in Tanjung Formation coals predominantly exceeded 5 μm in size and interpreted redox conditions in the water column during deposition as dysoxic, with some sulfide production in pore-waters.

2.1.3. Depositional setting of the Posidonienschiefer

All data for the Toarcian (Lower Jurassic) Posidonienschiefer in this study are taken from Indraswari et al. (*submitted*) that used one sample from a relative depth of 34.65 m in core A. This sample is thermally immature (0.5 % Ro, T_{max} 437 °C) and rich in organic matter. The Posidonienschiefer is a prolific hydrocarbon source rock in the Lower Saxony Basin of Northern Germany. This sequence is interpreted to have been deposited in an euxinic (free H_2S in the water column) marine environment based on the size distribution of framboidal pyrite, with limited terrestrial detrital and organic-matter input (Röhl et al., 2001; Schmid-Röhl et al., 2002; Frimmel et al., 2004; Schwark and Frimmel, 2004; Gorbanenko and Ligouis, 2014, 2015; Celestino et al., 2024). The selected sample has a total organic carbon (TOC) value of 8.85 % and a hydrogen index (HI) of 701 mgHC/g TOC.

2.2. Methods

Experimental setups follow those detailed in Indraswari et al. (*submitted*). In short, aliquots of ~6 g each of the Belemnite Marls and Tanjung Formation coal were solvent-extracted and subsequently analysed for Hg concentrations and Rock-Eval measurements before pyrolysis (outlined below). Each of the ~6 g solvent-extracted samples of Belemnite Marls and Tanjung Formation coal were divided into six sub-samples, resulting in a total of 12 sub-samples. Each sub-sample weighed approximately 1 g and was loaded into clean glass tubes to be heated in the furnace following Tannenbaum and Kaplan (1985), Lu and Kaplan (1989), and Dickson et al. (2020). Each glass tube was flame-sealed after removing atmospheric air to ~10^{-2} bar using a vacuum extraction line. The removal of air in the vessels to 10^{-2} bar was to prevent combustion / oxidation of the organic matter at the high temperatures of the pyrolysis, as under natural maturation conditions in the earth, there is little or no oxygen to react with in the sediments. Each sub-sample was put into a stainless-steel jacket and heated in the furnace isothermally at 325 °C for either 1 day, 7 days, 2 weeks, 3 weeks, or 5 weeks. After heating according to the designated time, each sub-sample was opened instantly to let the gaseous component out. The sediments, after heating, were solvent-extracted again to isolate the bitumen that evolved during thermal maturation. After centrifugation, the bitumen and solvent-extracted residues were separated and dried under N_2. The extracted rock residues were subsequently re-homogenized before Hg and Rock-Eval analyses. The bitumen generated during pyrolysis was extracted, dried under nitrogen and weighed, then re-dissolved and homogenized in dichloromethane (DCM): methanol (MeOH) (9:1, volume/volume) prior to Hg analyses.

2.2.1. Solvent extraction

Solvent extraction of the sediments before and after pyrolysis was undertaken using an Analytix Advanced Microwave Digestion System at the University of Oxford, following methods described in O'Connor et al. (2019). Before pyrolysis, existing free hydrocarbons were solvent-extracted from ~6 g sub-samples using 120 mL of DCM:MeOH (9:1, *v/v*). The microwave temperature settings were configured to gradually rise from room temperature to 70 °C in 10 min, isotherm at 70 °C for 10 min, and then decrease to 25 °C over 20 min. The sub-samples were then centrifuged and the sediments were separated from the solvent. The sediments were dried under a N_2 stream and divided into glass tubes for the pyrolysis experiment. After pyrolysis, each sub-sample of ~1 g was solvent-extracted using 20 mL of dichloromethane (DCM)/methanol (9:1, v/v). After centrifugation, the bitumen and solvent-extracted residues were separated and dried under N_2 to be analysed for Hg concentrations and Rock-Eval measurements.

2.2.2. Rock-Eval analysis

Analysis using the Rock-Eval 6 at the University of Oxford (Behar et al., 2001) was performed on solvent-extracted samples prior to pyrolysis and solvent-extracted sub-samples after pyrolysis. This analysis returns data on the total organic carbon (TOC), pyrolysable carbon in the rocks (S2, in mg HC per g rocks), hydrogen index (HI), and oxygen index (OI) in the sub-samples before and after pyrolysis. HI values are calculated as (100 × S2)/TOC (mg HC per g TOC). The HI is then used to determine the thermal maturity parameter as a simplified transformation ratio (TR), defined as $[(HI_{original} - HI_{measured})/HI_{original}]$. The reproducibility of the measurements was monitored using in-house standard SAB134 (Lower Jurassic organic-rich marl from St. Audries Bay, Somerset, UK, 2.7 % TOC and HI 660 $mgCO_2$/gTOC) for every 8 to 10 samples. The standard deviation of the in-house standard over the period of analysis (SAB134) was ±0.1 % TOC and ± 15 mgHC/gTOC for HI.

2.2.3. Mercury analysis for sediments and bitumen

Mercury (Hg) concentration analyses for solvent-extracted sediments before and after pyrolysis were conducted with a Lumex RA 915 M device, attached to a pyrolysis unit (PYRO-915+) at the University of Oxford (Bin et al., 2001). Powdered sub-samples of 50 ± 5 mg in sample boats were rapidly heated from ~20 to ~700 °C, during which Hg was released. Before each run, the instrument was calibrated using NIST-SRM2587 (National Institute of Standards and Technology – Standard Reference Material: Trace Elements in Soil Containing Lead from Paint), with a mercury (Hg) concentration of 290 ± 9 ppb. The long-term analyses of the SRM2587 standard indicate reproducibility of Hg concentration within ±5 % of the measured value. The manufacturer-specified detection limit for the Lumex RA 915 M is ~0.05–0.1 ng Hg for solid samples weighing 100–200 mg (0.5–1 ng g^{-1} or ppb by weight).

Mercury concentrations in bitumen were also analysed using a Lumex RA-915 M, following methods similar to those used for oil analysis as detailed in Indraswari et al. (2024; *submitted*). After pyrolysis, the solvent-extractable fractions (bitumen) were isolated (§2.2), dried under a nitrogen (N_2) stream, and the solvent-free weight of each bitumen sub-sample was recorded. Before Hg analysis, the bitumen was redissolved and homogenized in 9:1 (v:v) DCM:MeOH. A 250 μL aliquot of the diluted bitumen was pipetted into a quartz boat, dried under nitrogen, and weighed. A food-grade activated charcoal bed was added to minimize oil smoke interference in Hg analyses. Mercury concentrations in the activated charcoal were also analysed to correct bitumen data for trace Hg present in the charcoal bed, with repeat measurements ($n = 15$) showing an average concentration of 0.44 ± 0.06 ppb (standard error of the mean), equating to 0.044 ± 0.006 ng Hg for a 100 mg charcoal bed. Finally, duplicate measurements of Hg concentration in each bitumen sub-sample were taken, with the trace Hg from the charcoal bed subtracted to obtain accurate Hg estimates in the bitumen fraction.

2.2.4. Thermal desorption profiles (TDPs) for mercury

Thermal desorption profiles (TDPs) for sedimentary Hg from solvent-extracted sediments before and after pyrolysis were obtained using a Lumex RA-915 M set up with a PYRO-915+ at the University of Oxford, according to the procedures described in Frieling et al. (2024). These TDPs allow us to examine whether changes in Hg speciation occur in the sediment residues during maturation. The desorption profiles were obtained concurrently with the total mercury concentration measurements

within the pyrolysis chamber in Mode 1 (stable temperature of ~700 °C). The weight of each sample was held constant at 50 ± 5 mg to avoid the effects of variable sample mass.

In addition to the standard desorption procedure, we conducted a preliminary assessment to ensure that the Tanjung coal sample did not undergo self-ignition during heating. Saniewska and Bełdowska (2017) reported that samples with high organic matter content (Loss on Ignition (LOI) > 20 %, approximately > ~ 9.4 % TOC) may spontaneously combust between 225 and 250 °C. Given that one of the samples is coal which has a high TOC, we gradually heated it from 150 °C to 300 °C in 25 °C increments, holding each step for 5 min, using a Lumex 915Lab at the University of Oxford. The temperature of the combustion cell was continuously monitored throughout. No anomalous temperature increases were observed, indicating the sample remained stable and was suitable for subsequent Hg measurements.

3. Results

3.1. Organic-matter maturation

3.1.1. Initial conditions

We conducted new measurements on sub-samples of the Belemnite Marls and the Tanjung Formation coal. The untreated sub-sample of Tanjung Formation coal has a high hydrogen index (HI) of 290 mg HC/g TOC and a low oxygen index (OI) of 16 mg CO_2/g TOC. By contrast, the original untreated Belemnite Marls sub-sample has a lower HI value of 100 and a higher OI value of 125.

3.1.2. Effects of maturation on OM characteristics

The effect of artificial thermal maturation on the three different samples is shown in Table 2 and the modified van Krevelen diagram (Fig. 2A). The maturation of all samples with increasing heating time is demonstrated, as expected, by the reduction in the HI, as a result of transformation of kerogen into bitumen and gas. Compared to the original HI values for the samples, the decrease in HI is 55 % for the Posidonienschiefer, 36 % for the Tanjung Formation coal and 68 % for the Belemnite Marls. However, it is important to note that the original HI of the Belemnite Marls is already quite low prior to maturation and the longer experiments result in S2 peaks near the analytical limit for quantification (0.2 mg HC/g). The Posidonienschiefer experienced the largest relative TOC loss, with a 32 % reduction from its original TOC of 8.85 wt% to 6.07 wt% (Fig. 2B). The loss of TOC in Tanjung Formation coal is minimal, with a 3 % relative reduction from its initial TOC value. In the Belemnite Marls, all sub-samples showed variations within analytical error (Table 2, Fig. 2B).

3.2. Mercury (Hg) and Hg/TOC in residues and bitumen

All three samples (the Posidonienschiefer, the Belemnite Marls, and the Tanjung Formation coal) show systematic Hg loss with increasing pyrolysis times, but to different degrees. The original untreated Belemnite Marls sub-sample has an initial total Hg (Hg_T) concentration of 325.4 ppb and the sub-sample heated after 840 h lost ~83 % of its Hg_T (Table 2, Fig. 3). The original untreated Tanjung Formation coal sub-sample has an initial Hg_T concentration of 44.2 ppb and the 840-h sub-sample shows a loss of 93 % of the initial Hg_T. The previously analysed original untreated Posidonienschiefer sub-sample has an initial Hg_T concentration of 74.6 ppb (Indraswari et al. *submitted*) with 63 % initial Hg_T loss after 840 h heating. Because of the different rates of change of TOC and Hg_T in the sample sets through the pyrolysis experiments, we also observe a distinct decrease in Hg_T/TOC in all samples (Table 1 and Fig. 3B). The Belemnite Marls sub-samples showed a reduction in Hg_T/TOC from ~383 ppb/% (0 h heating) to ~67 ppb/% (840 h heating) whereas the Tanjung Formation coal started with 1.79 ppb/% Hg/TOC in the non-heated sub-sample and ended up with 0.22 ppb/% Hg/TOC in the sub-sample heated after 840 h. The Posidonienschiefer started with an initial Hg_T/TOC of 8.43 ppb/% in the original sub-sample and declined to 4.70 ppb/% after 840 h of pyrolysis.

Clear differences between the sample types appear when examining the rate of Hg_T loss over heating time. The rate of Hg_T loss, especially after the first 24 h of isothermal heating, is similar for the Belemnite Marls and the Tanjung Formation coal, with the Belemnite Marls having 24 % of Hg_T retained in the sediment residue and the Tanjung Formation coal 29 % (Fig. 3C, Table 3). By contrast, the Posidonienschiefer retained 64 % of Hg_T after 24 h heating, signifying a much slower Hg release. Continued isothermal heating of the Posidonienschiefer resulted in progressive Hg loss but at a reduced rate compared to that of the first 24 h (Fig. 3C) reaching a minimum of 30 % at 500 h. The Tanjung Formation coal also still continued to release Hg after the first 24 h (~10 % Hg_T retained after 500–840 h heating) while the Belemnite Marls experienced only a more subtle decrease (17 % of the original Hg_T after 840 h of heating) (Fig. 3C).

The amount of bitumen produced after heating for each sub-sample varies (Fig. 4A). There is an observed trend of increasing bitumen mass produced in the more mature sub-samples for the Posidonienschiefer and Tanjung Formation coal. On the other hand, the Belemnite Marls, with a high proportion of inert OM (type IV kerogen), produced no bitumen during heating. In the earlier stage of maturation level (TR < 0.3), the Posidonienschiefer generated a slightly higher amount of bitumen (~15 mg bitumen/g sediment, Indraswari et al., submitted) compared to the Tanjung Formation coal (~13 mg bitumen/g sediment, Table 3). However, at the higher maturity level (TR ~0.4), both the Posidonienschiefer and the Tanjung Formation coal generated a similar amount of bitumen: 22–23 mg/g sediment (Fig. 4A).

The results of Hg concentration measurements in the bitumen from the Tanjung Formation coal corresponding to its transformation ratio are shown in Fig. 4B. These results plotted together with the ones from the Posidonienschiefer (Indraswari et al., submitted) show the absence

Table 2
The geochemical measurements from Tanjung Formation coal and Belemnite Marls analysed in this study (also shown in Figs. 1 and 2). HI: Hydrogen Index. OI: Oxygen Index. TOC: Total Organic Carbon. TR: transformation ratio, change in Hydrogen Index during pyrolysis, defined as $[(HI_{original} - HI_{measured})/HI_{original}]$. T_{max}: temperature of maximum hydrocarbon yield during pyrolysis. S2: pyrolysable carbon in the rocks.

Sample	Heating time (hour)	HI (mg HC/g TOC)	OI (mg CO_2/g TOC)	TOC (%)	TR	T_{max} (°C)	S2 (mg HC/g rock)	Total Hg (ppb)	Hg/TOC (ppb/%)
Tanjung Formation coal	0	290	16	24.7	0	428	68.76	44.2	1.79
	24	240	7	24.3	0.17	432	58.29	12.7	0.52
	336	208	5.5	24	0.28	439	49.78	10.8	0.45
	500	187	4	24.3	0.36	446	45.44	3.6	0.15
	840	226	5	24.3	0.22	437	54.47	5.4	0.22
Belemnite Marls	0	100	125	0.85	0	432	0.85	325.4	382.76
	24	75	63	0.81	0.25	433	0.61	78.7	97.16
	168	65	51	0.82	0.35	437	0.53	65.9	80.37
	336	75	54	0.8	0.25	437	0.6	74.7	93.38
	500	56	53	0.79	0.44	439	0.44	60.8	76.96
	840	32	45	0.82	0.68	439	0.26	55.3	67.44

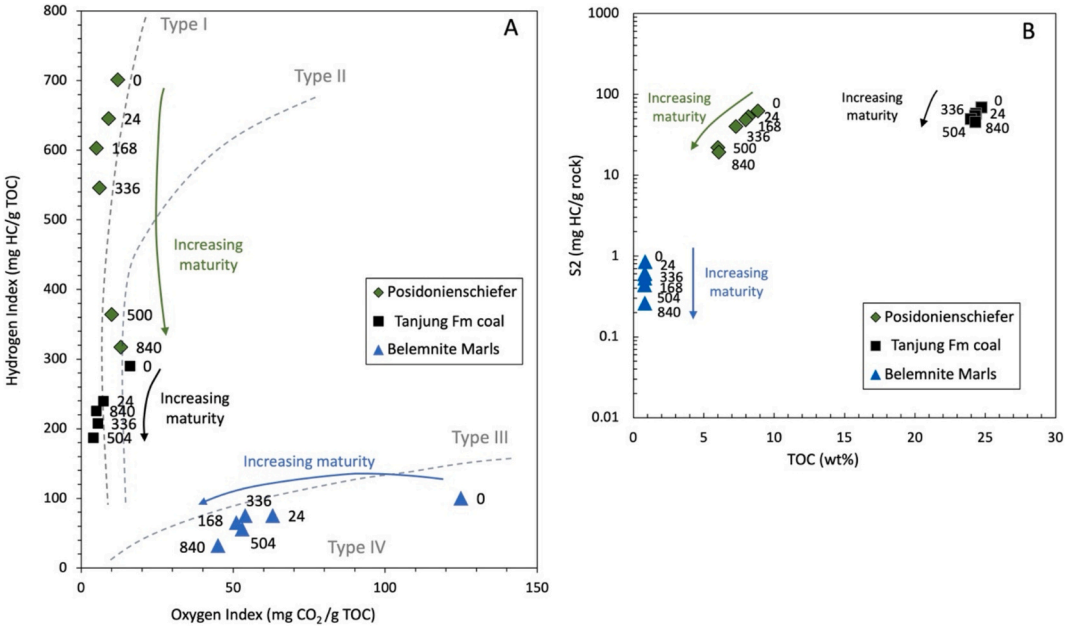

Fig. 2. A. Modified van Krevelen diagram showing the maturity evolution of samples in this study. **B.** S2-TOC plot showing S2 decrease as samples mature for all samples. Number labels by points show heating time in hours.

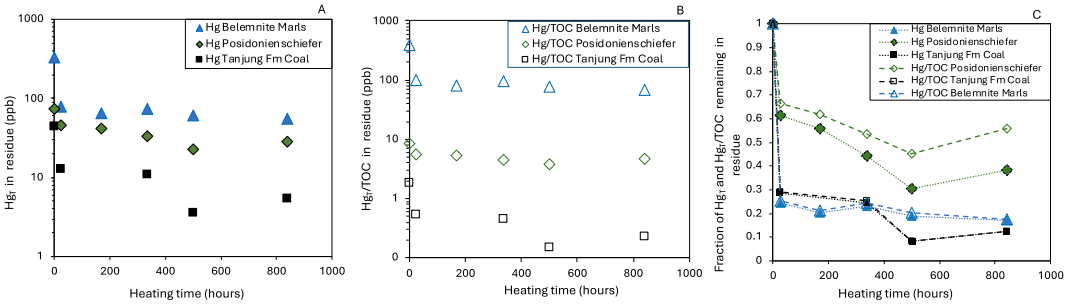

Fig. 3. A. Total Hg (Hg_T) concentration remaining in the residue after pyrolysis. **B.** Hg_T/TOC in the residue. **C.** Fraction of Hg_T and Hg_T/TOC of the original Hg_T concentration and original Hg_T/ TOC in the residue. Note that the y-axes in A and B are logarithmic. The Posidonienschiefer data is from Indraswari et al. (2025).

Table 3
Distribution of Hg in the residues and bitumen from the Tanjung Formation coal analysed in this study (also shown in Fig. 4). HI: Hydrogen Index. TOC: Total Organic Carbon. T_{max}: temperature of maximum hydrocarbon yield (S2) during pyrolysis. TR: transformation ratio (change in Hydrogen Index during pyrolysis). Extracted Residue: pyrolysed bulk-rock residue after solvent extraction. Bitumen: the total solvent-extractable organic matter. The gas loss is calculated using the difference: Hg loss as gas = 100 % − %Hg in bitumen − %Hg in the sediments. N.D.: not determined. No measureable amount of total lipid extract (TLE) could be obtained from the Belemnite Marls.

Sample	Heating time (hours)	HI (mg HC/g TOC)	TOC (%)	TR	TLE (mg/g sediment)	Total Hg				
	0	290	24.7	0	0.16	44.2 ppb				
						Extracted Residues		Bitumen		Loss (as gas)
							% of Total		% of Total	% of Total
Tanjung Formation coal						ppb	Hg	ppb	Hg	Hg
	24	240	24.3	0.17	7.55	12.70	28.73	66.35	0.14	71.13
	336	208	24	0.28	12.61	10.80	24.43	94.25	0.77	74.80
	500	187	24.3	0.36	22.08	3.60	8.14	86.45	0.81	91.04
	840	226	24.3	0.22	10.35	5.40	12.22	30.15	0.06	87.72
	0	100	0.85	0	–	325.4 ppb				
						Extracted Residues		Bitumen		Loss (as gas)
							% of Total		% of Total	% of Total
Belemnite Marls						ppb	Hg	ppb	Hg	Hg
	24	75	0.81	0.25	–	78.7	24.19	n.d.	0	75.81
	168	65	0.82	0.35	–	65.9	20.26	n.d.	0	79.74
	336	75	0.8	0.25	–	74.7	22.96	n.d.	0	77.04
	500	56	0.79	0.44	–	60.8	18.69	n.d.	0	81.31
	840	32	0.82	0.68	–	55.3	17.00	n.d.	0	83.00

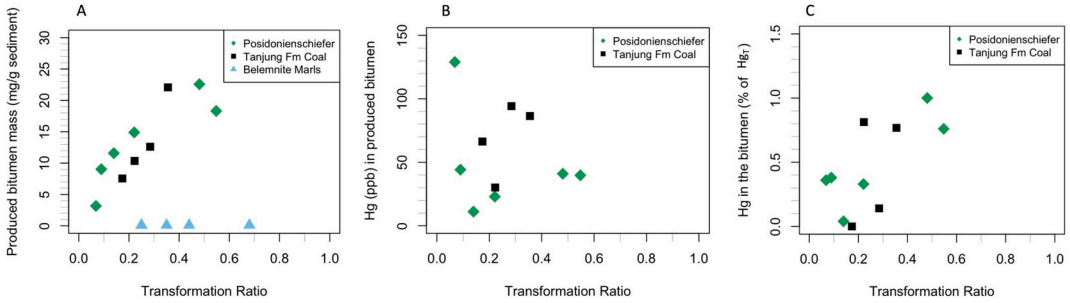

Fig. 4. **A.** Bitumen mass produced from heated samples in this study with respect to their transformation ratio. There is an observed trend of increasing bitumen mass produced in the more mature samples for the Posidonienschiefer and Tanjung Formation coal sub-samples. The Belemnite Marls sub-samples did not generate enough bitumen for Hg analyses. **B.** Mercury concentration in the produced bitumen from pyrolysis. **C.** Fraction of Hg (% of Hg_T) in the original samples partitioned to the bitumen.

of a strong correlation between Hg concentration in the bitumen and maturity level. When the proportion of the Hg mass in the bitumen is calculated from the Hg_T, we find that the percentage of mercury that partitioned into the bitumen after pyrolysis ranges from 0.05 % to 0.8 % of the initial Hg_T in the Tanjung Formation coal, similar to what is observed for the Posidonienschiefer (0.04 %–1 %) (Indraswari et al., submitted) (Fig. 4C).

3.3. Thermal desorption profiles (TDPs) of sedimentary mercury

The thermal desorption profiles (TDP) show Hg release over time (seconds) as the sample is heated in the furnace during Hg concentration analysis. Frieling et al. (2024) proposed that the relatively low-temperature Hg release peak relates to Hg bound to organic matter (OM) or OM-associated sulfides, and the later release as other Hg release phases (which may include, e.g., red HgS (cinnabar)). We follow the

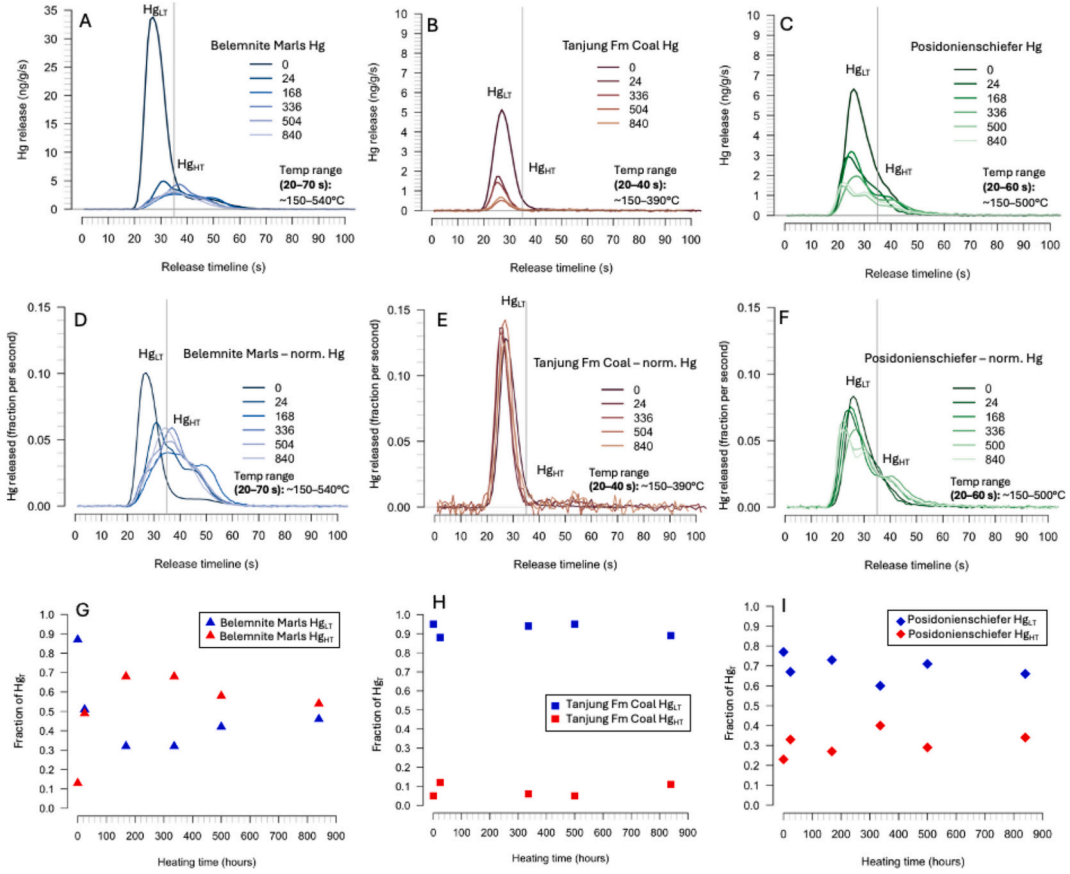

Fig. 5. Thermal desorption and Hg release intensity for samples before and after pyrolysis (number labels by lines show heating time in hours). While the exact temperature for each time point cannot be directly calibrated due to variability in organic composition, from thermocouple run of 100 mg silica powder, we estimate that Hg release begins at ~150 °C (around 20 s) and completes before ~540 °C (around 70 s) in Belemnite Marls sample. **A.** Hg release (in ng g^{-1} s^{-1}) for the Belemnite Marls sub-samples. **B.** as panel A for the Tanjung Formation coal. **C.** as panel A for the Posidonienschiefer from Indraswari et al. (*submitted*). **D.** Hg release intensity for the Belemnite Marls sub-samples, normalized to the total Hg release (Area) from each sub-sample. **E.** As panel D for the Tanjung Formation coal. **F.** As panel D for the Posidonienschiefer from Indraswari et al. (*submitted*). **G.** Fraction of low-temperature Hg (Hg_{LT}) and high-temperature Hg (Hg_{HT}) – defined by their release stage with Hg_{LT} released first and Hg_{HT} released later in the TDP – compared to the heating time for the Belemnite Marls sub-samples. **H.** as panel G for the Tanjung Formation coal. **I.** as panel G for the Posidonienschiefer.

same methodological approach as Frieling et al. (2025), who used a cut-off to separate the distinct low-temperature Hg phase (Hg_{LT}) from the higher temperature Hg phases (Hg_{HT}) (note that $Hg_{LT} + Hg_{HT} = Hg_T$) to illustrate how Hg speciation relates to Hg mobilization in the vicinity of a contact aureole. Here we use a cut-off at 35 s. The Hg-TDP results from the Posidonienschiefer, the Belemnite Marls, and the Tanjung Formation coal used in this study show distinct behaviour in Hg release as a response to isothermal heating in the experimental pyrolysis (Fig. 5). Each curve in Fig. 5A, B, and C represents Hg release (in ng per gram of sample material) per second and the curves in Fig. 5D, E, and F show the fraction of Hg released per second, normalized to the total Hg release for each sub-sample.

3.3.1. Belemnite Marls Hg behaviour

In the original untreated (i.e., prior to artificial maturation) Belemnite Marls sub-sample, a prominent Hg release peak occurs around 30 s (Fig. 5A, darkest blue line), which is likely associated with OM based on its position early in the TDP (Frieling et al., 2024)(). After 24 h of heating, however, this Hg release peak is no longer prominent, and the maximum Hg release significantly decreases from 35 ng/g/s to 5 ng/g/s, which corresponds with the reduction in Hg concentration observed in the 24-h sub-sample (Fig. 3, Table 3). The concentration-normalized plot of Belemnite Marls sub-samples heated for ≥24 h shows a delayed and more prolonged Hg release (Fig. 5D), with a consistent release profile across these sub-samples and only minimal further reduction in Hg release (Fig. 5A, D). This sharp decrease in the early, lower temperature Hg release phase (Hg_{LT}) indicates that this is the dominant phase that was volatilized in the first 24 h of isothermal maturation, while the sub-samples that were heated for longer show a later, more stable peak, around 40 s and strongly reduced rate of Hg loss.

Before maturation, the Belemnite Marls sub-sample is dominated by the low-temperature Hg phase, with 87 % Hg_{LT} and 13 % Hg_{HT} (Fig. 5G). After 24 h of heating, the proportion of Hg_{LT} to Hg_{HT} in the Belemnite Marls sub-sample changed to 51:49. This ratio subsequently exhibited slight fluctuations in the proportion, with Hg_{HT} making up 68 %, 58 %, and 54 % after 336, 500, and 840 h of heating, respectively.

3.3.2. Tanjung Formation coal Hg behaviour

For the Tanjung Formation coal, the Hg release signals from the untreated sub-sample show a single peak (Fig. 5B). The signals from the heated (≥ 24 h) sub-samples are identical to the untreated sub-sample but with lower overall Hg concentrations (Fig. 5B, E, Table 3). This characteristic is further demonstrated in the normalized plots of the Tanjung Formation coal sub-samples (Fig. 5E), which show identical and overlapping curves, with all sHg released at broadly the same intensity (max ≥0.1 fraction/s at second 30).

The proportion of Hg phases in the Tanjung Formation coal began at 95:5 Hg_{LT}:Hg_{HT} in the original untreated sample (Fig. 5H). Only a very subtle change in the proportion of Hg phases was observed during heating, as the proportion of Hg_{LT} and Hg_{HT} in the Tanjung Formation coal sub-samples remained nearly stable at approximately 90:10 after heating for 24 to 840 h.

3.3.3. Posidonienschiefer Hg behaviour

The original Posidonienschiefer sub-sample appears to yield a dominant, single-phase Hg release peak. However, Hg release is more prolonged compared to the main Hg release peak of the Belemnite Marls and the Tanjung Formation coal (Fig. 5A, B, C), indicating the presence of a Hg_{HT} phase. In contrast to the Belemnite Marls sub-samples that lost most of their Hg_{LT} after heating, the heated sub-samples of the Posidonienscheifer still show a main Hg peak release relatively early in the TDP (<30s). The heated sub-samples of the Posidonienschiefer (≥ 24 h) display more complex TDPs, featuring bimodal peaks and 'shoulders', further supporting the presence of multiple Hg species (Fig. 5C, F).

Examining the distribution of Hg phases, the original Posidonienschiefer sub-sample exhibits a higher proportion of Hg_{HT} compared to the previously described samples, with a 77:23 ratio of Hg_{LT}:Hg_{HT} (Fig. 5I). Similar to the Tanjung Formation coal, the proportion of Hg phases in the Posidonienschiefer shows only subtle changes after heating, at approximately 70:30 Hg_{LT}:Hg_{HT}.

4. Discussion

In this study, we analysed two very different distinct sedimentary rocks, each representing different depositional environments and organic-matter (OM) types, and compared to another recently studied sample (Indraswari et al., submitted) from another depositional setting and environment. The Belemnite Marls sample is an example of a calcareous marine mudrocks, dominated by relatively inert organic carbon, that contains pyrite due to low oxygen (dysoxic) conditions at the sediment-water interface upon deposition and potentially sulfidic conditions in pore waters after sulfate reduction (Schöllhorn et al., 2020). The Tanjung Formation coal is a lignin-rich coal deposited in a less reducing fresh-water-dominated environment, where sulfate and particularly sulfides are scarce, and organic matter predominantly consists of plant-derived material. As described in Indraswari et al. *(submitted)*, the Posidonienschiefer is a marine, highly organic-rich black shale, formed under euxinic conditions where sulfide was abundantly available in both the water column and sediment.

After isothermal heating of varying durations, distinct patterns of Hg loss emerged across the three lithologies, with the rate of Hg release being highest within the first 24 h of heating at 325 °C. The Belemnite Marls and Tanjung Formation coal released more than 70 % of their Hg_T during this initial period, whereas the Posidonienschiefer exhibited slower Hg release, with only 40 % of Hg_T volatilized (Fig. 3). These findings align with trends observed in similar experiments from previous studies (Liu et al., 2022; Chen et al., 2022), which also showed variations in Hg_T release efficiency. For example, clastic marine shales demonstrated less efficient Hg_T release curves compared to calcareous marine and lacustrine shales (Fig. 1).

4.1. Is the rate of Hg release from sediments related to different primary Hg speciation characteristics?

The mercury thermal desorption profiles (TDPs) of the samples allow us to see distinct differences in Hg phase stability across the three sediment types (Fig. 5A-F). These differences in Hg release rates can be directly linked to the Hg speciation in the sub-samples before heating and are illustrated as changes in the relative proportions of low-temperature (Hg_{LT}) and high-temperature (Hg_{HT}) phases (Fig. 5G, H, I). The rapid Hg_T release observed during the first 24 h of heating in the Belemnite Marls and Tanjung Formation coal (Fig. 3C) corresponds closely to the dominance of the Hg_{LT} in these sub-samples. Specifically, the original sub-samples of the Belemnite Marls and Tanjung Formation coal with 87 % and 95 % Hg_{LT}, respectively, make the sedimentary Hg more susceptible to volatilization upon relatively modest heating. The TDPs further illustrate the fact that the Belemnite Marls exhibit single-phase release patterns dominated by the loss of Hg_{LT} in the first 24 h (Fig. 5A). For the Tanjung Formation coal, the position of the Hg release peak from the original sample suggests most Hg is present as Hg bound to OM or OM-associated sulfides (Frieling et al., 2024). Moreover, the plots of the Tanjung Formation coal indicate that this Hg phase remains dominant throughout the heating experiment, despite a decreasing concentration (Fig. 5B).

By contrast, the slower Hg_T release observed in the Posidonienschiefer during the first 24 h (Fig. 3C) is consistent with its higher proportion (> 20 %) of more thermally stable (Hg_{HT}) species prior to heating (Fig. 5I) compared to the Belemnite Marls (~13 %, Fig. 5G) and Tanjung Formation coal (<10 %, Fig. 5H). The Hg_{HT} complexes, which may include, for example, cinnabar (desorption temperature > 275 °C vs Hg-OM > 225 °C; Rumayor et al., 2015; Saniewska and Bełdowska, 2017) are more thermally stable than Hg

associated with organic matter, making them less prone to volatilization during heating.

4.2. Sedimentary Hg speciation and primary depositional environment

The factors influencing Hg speciation in recent soft sediments have been extensively studied, including sulfur availability (e.g., Benoit et al., 1999; Fabbri et al., 2001), particle size variations linked to depositional environments (e.g., Boszke et al., 2004; Xu et al., 2021), and the proximity of depositional sites to pollution sources in modern settings (e.g., Wallschläger et al., 1998; Bindler et al., 2001). In this study, the samples primarily differ in their depositional settings, allowing us to investigate how the sedimentary environment may have influenced primary Hg speciation and how this characteristic ultimately may have affected Hg behaviour during heating.

The Posidonienschiefer, characterized by a high proportion of Hg_{HT}, was deposited under euxinic conditions. In such environments, the uptake potential of Hg by sulfides is significantly enhanced due to the stronger chemical affinity of Hg^{2+} for sulfide (S^{2-}) compared to organic matter (Ravichandran, 2004; Bower et al., 2008). These conditions provide abundant sulfide, thereby enabling Hg and other metals to bind and form sulfide minerals. This process may then result in a higher proportion of sulfide-bound or sulfide-hosted Hg in strata such as the Posidonienschiefer. If part of the Hg is present as cinnabar HgS, this may explain the larger proportion of Hg_{HT} compared to the other successions examined here. Similarly, the Belemnite Marls exhibit evidence of a substantial quantity of Hg_{HT}, in the original sample that becomes more significant after the isothermal heating process. While this may seem unexpected as the depositional environments were quite different in their oxidation regime, the presence of similar Hg phases could be attributed to the potential for sulfate reduction and sulfide production in pore waters in the Belemnite Marls sequence. Despite the dysoxic bottom-water conditions, the Belemnite Marls commonly contain some pyrite, likely deposited in sulfidic pore-waters. By contrast, the Tanjung Formation coal, deposited in a less reducing and notably low-salinity (fresh-water-dominated) environment, does not show a substantial proportion of Hg_{HT}. Thus, we may speculate that there may have been minimal sulfide available for Hg to bind with even in the more anoxic pore waters, leading to Hg being almost exclusively associated with OM. Despite the major differences in primary Hg speciation related to the environment of deposition and potential for the formation of sulfide minerals, both the Belemnite Marls and Tanjung Formation coal released Hg_T at similar efficiency in the first 24 h of heating, which can be attributed to the dominance (~90 %) of relatively low-temperature fractions of Hg, likely OM-associated Hg, in both these original untreated samples.

Although we cannot examine the TDPs for previously published maturation experiments, we postulate that the differences in Hg behaviour between the sample types in the previous studies of thermal maturation by Liu et al. (2022) and Chen et al. (2022) also reflect variations in the availability of sulfur and the type of OM present during deposition. The efficiency of Hg volatilization in sedimentary rocks deposited in marine euxinic environments, such as the Proterozoic Xiamaling Formation (Liu et al., 2022) and the Cryogenian Datangpo Formation (Chen et al., 2022), aligns with our observations in the Posidonienschiefer (green asterisk in Fig. 1). Similarly, the Permian Talung Formation, which is a calcareous shale (Liu et al., 2022) exhibits the efficiency of Hg loss comparable to that recorded in the Belemnite Marls (Fig. 1). These findings suggest that depositional environments and early diagenesis play a crucial role in determining the proportion of organic-bound and higher temperature (potentially sulfide-mineral-associated) Hg. We therefore consider it likely that the differences of Hg loss between these sample types in the studies by Chen et al. (2022) and Liu et al. (2022) (Fig. 1) are, at least in part, explained by differences in initial Hg speciation, which in turn is related to the depositional environment from which the samples derive.

This study highlights that in sedimentary rocks with Hg_{HT} complexes (sulfur-rich), Hg volatilization during heating can be substantially suppressed compared to non-sulfur-rich lithologies. As such, understanding the sulfur content and speciation of the source rocks is critical when attempting to calibrate or model Hg/C emission ratios, especially in the context of LIP-driven volatile release.

4.3. Thermally induced organic matter transformation and Hg release

The nature of organic matter (OM) available as a potential host phase for Hg has an influence on the type of products generated and released during thermal maturation and may also affect the mobilization and transport of Hg. The terrestrially sourced Tanjung Formation coal is mainly a gas-prone source rock, although it also generates bitumen due to its exceptional content of oil-prone liptinitic components (Davis et al., 2007; Kusuma and Darin, 1989). By contrast, marine OM, rich in oil-prone algal and bacterial biomass, such as the Posidonienschiefer, will generate a significantly higher proportion of liquid products relative to gas (Tissot and Welte, 1984). This observation is especially relevant in the maturity range of our isothermal pyrolysis experiments that rather simulate the early to peak oil-generative phases (0.6–0.9 % Ro) without extending into the gas window. Hence, the mobilization of Hg during thermal maturation of these different types of labile organic matter (Tanjung Formation coal and Posidonienschiefer), may be impacted by the relative amount of gas or liquid phases generated, with more efficient transport in the gas. By contrast, the Belemnite Marls sub-samples used in our study has little, if any, labile organic matter and is unlikely to generate cracking products that would be involved in or facilitate the transport of Hg. The trends of Hg_T loss we observe in the various experimental heating intervals (after 24, 168, 336, 500, and 840 h) in the Posidonienschiefer and Tanjung Formation coal (Fig. 3C) could consequently be related to the variable production of bitumen and hydrocarbon gas from the two different types of OM. Crucially, the processes that drive hydrocarbon formation and mobilize fluids in the subsurface may be critical for Hg mobilization after release from its original host phase. However, this hypothesis remains speculative, and further research is needed to more fully understand the mechanisms by which hydrocarbon formation and subsurface fluid mobilization contribute to Hg mobilization after release from its host phase.

4.4. Relevance to contact aureoles and burial-related maturation

In the contact aureoles associated with LIP dykes, various types of sedimentary rocks are intruded, ranging from organic-rich (e.g., Ecca group in Karoo basin: Aarnes et al., 2011; Svensen et al., 2007, 2015) to organic-lean sedimentary rocks (e.g., evaporites in Siberian Traps and the CAMP: Svensen et al., 2009; Heimdal et al., 2018). The amount of Hg volatilized and released from these contact aureoles is influenced by the type of sedimentary rocks intruded. For example, this study suggests that sedimentary rocks deposited in less reducing environments with limited sulfide, release Hg more efficiently when heated compared to those deposited under marine anoxic to euxinic conditions. This finding implies that we must be cautious in using Hg release to back-calculate carbon emissions, for example, as it requires careful consideration of the Hg speciation composition influenced by sedimentary depositional settings.

Similar factors apply to thermal maturation in natural systems related to burial or subsidence. For example, our findings support the proposal that the immobility of Hg in the naturally matured Posidonienschiefer samples (Cores B and C) observed by Indraswari et al. (2024) can be explained by the inefficiency of Hg volatilization, likely in part due to the high proportion of Hg_{HT} in the immature core (Core A; Fig. 5) that further increases with maturation in Cores B and C (Indraswari et al., submitted).

In summary, our findings highlight the critical importance of understanding sedimentary Hg speciation distribution (e.g., high-

temperature versus low-temperature species) in immature rocks to aid the interpretation of the effects of thermal maturation in natural systems, both burial- and intrusion-related. These findings also underscore the need to account for lithological differences when interpreting Hg signal changes due to thermal maturation—especially in non-organic-rich sediments, where most Hg anomalies interpreted as LIP proxies have been observed. Expanding the geochemical framework to include such lithologies is essential for improving paleoenvironmental reconstructions and for accurately assessing Hg mobility across diverse depositional environments.

5. Conclusions & outlook

In order to improve understanding of the behaviour or mercury during thermal maturation of sedimentary rocks, we conducted pyrolysis experiments involving isothermal heating at 325 °C for varying durations (24–840 h) on two sedimentary rocks, each representing different depositional environments and organic-matter (OM) types: the calcareous marine mudrocks of the poorly oxygenated shallow-marine Belemnite Marls and the Tanjung Formation coal from a coastal swamp. These materials were analysed and compared with the marine anoxic to euxinic Posidonienschiefer, which underwent the same experimental treatment in a previous broader study (Indraswari et al., submitted). We observe significant variability in Hg release efficiency, which we link to the initial Hg speciation (proportion of high-temperature stable Hg (Hg_{HT}) vs low-temperature stable Hg (Hg_{LT}) species) of the samples using thermal desorption profiles (TDPs). The TDPs reveal distinct differences in the Hg speciation between the Belemnite Marls sample (~13 % Hg_{HT}), Tanjung Formation coal (<10 % Hg_{HT}), and the Posidonienschiefer (>20 % Hg_{HT}). The depositional setting of the sediments appears to have influenced the initial Hg speciation, possibly via the availability of sulfide during and after deposition (in the water column and/or pore waters). These data directly connect the thermal stability of Hg phases to their volatilization potential after long-term exposure to heat. These results also suggest that the thermal desorption profiles (TDPs) can potentially be used to project the efficiency of Hg release under slow heating rates and isothermal conditions such as occur in deep basins and around igneous intrusions. Crucially, the differences in initial Hg speciation and resulting Hg release efficiency largely explain differences in Hg behaviour during isothermal heating in our sample set and may explain the significant differences in Hg loss observed within the sedimentary rock types in previous experiments (Liu et al., 2022; Chen et al., 2022) as well.

CRediT authorship contribution statement

Asri O. Indraswari: Writing – original draft, Visualization, Validation, Methodology, Investigation, Formal analysis, Data curation. **Joost Frieling:** Writing – review & editing, Validation, Supervision, Methodology, Data curation, Conceptualization. **Erdem Idiz:** Writing – review & editing, Validation, Supervision. **Tamsin A. Mather:** Writing – review & editing, Validation, Supervision, Funding acquisition. **Alexander J. Dickson:** Writing – review & editing, Validation, Supervision. **Hugh C. Jenkyns:** Writing – review & editing, Validation, Supervision. **Stuart A. Robinson:** Writing – review & editing, Validation, Supervision. **Isabel M. Fendley:** Writing – review & editing, Validation, Formal analysis. **Oliver Neilson:** Formal analysis.

Declaration of competing interest

The authors declare that they have no known competing financial interests or personal relationships that could have appeared to influence the work reported in this paper.

Acknowledgments

We thank S. Wyatt. and J. Brakeley for analytical assistance. Funding was provided from the European Research Council Consolidator Grant (ERC-2018-COG-818717-V-ECHO). A.I. is supported by a Jardine Foundation scholarship.

Data availability

Data is available on the link below.

Data for: The influence of primary depositional conditions on Hg behaviour during early thermal maturation (Original data) (Figshare)

References

Aarnes, I., Fristad, K., Planke, S., Svensen, H., 2011. The impact of host-rock composition on devolatilization of sedimentary rocks during contact metamorphism around mafic sheet intrusions. Geochem. Geophys. Geosyst. 12 (10). https://doi.org/10.1029/2011GC003636.

Anggara, F., Patria, A.A., Rahmat, B., Wibisono, H., Putera, M.Z.J., Petrus, H.T.B.M., Erviana, F., Handini, E., Amijaya, D.H., 2024. Signature characteristics of coal geochemistry from the Eocene Tanjung Formation and the Miocene Warukin Formation, Barito Basin: insights into geological control on coal deposition and future critical element prospection. Int. J. Coal Geol. 282, 104423. https://doi.org/10.1016/j.coal.2023.104423.

Baucon, A., Bednarz, M., Dufour, S., Felletti, F., Malgesini, G., Neto de Carvalho, C., Niklas, K.J., Wehrmann, A., Batstone, R., Bernardini, F., Briguglio, A., Cabella, R., Cavalazzi, B., Ferretti, A., Zanzerl, H., McIlroy, D., 2020. Ethology of the trace fossil Chondrites: form, function and environment. Earth Sci. Rev. 202, 102989. https://doi.org/10.1016/j.earscirev.2019.102989.

Behar, F., Beaumont, V., Penteado, De B., H. L., 2001. Rock-Eval 6 technology: performances and developments. Oil Gas Sci. Technol. 56 (2), 111–134. https://doi.org/10.2516/ogst:2001013.

Benoit, J.M., Gilmour, C.C., Mason, R.P., Heyes, A., 1999. Sulfide controls on mercury speciation and bioavailability to methylating bacteria in sediment pore waters. Environ. Sci. Technol. 33 (6), 951–957. https://doi.org/10.1021/es9808200.

Bin, C., Xiaoru, W., Lee, F.S.C., 2001. Pyrolysis coupled with atomic absorption spectrometry for the determination of mercury in Chinese medicinal materials. Anal. Chim. Acta 447 (1–2), 161–169. https://doi.org/10.1016/S0003-2670(01)01218-1.

Bindler, R., Renberg, I., Appleby, P.G., Anderson, N.J., Rose, N.L., 2001. Mercury accumulation rates and spatial patterns in lake sediments from West Greenland: a coast to ice margin transect. Environ. Sci. Technol. 35 (9), 1736–1741. https://doi.org/10.1021/es0002868.

Boszke, L., Sobczynski, T., Glosinska, G., Kowalski, A., Siepak, J., 2004. Distribution of mercury and other heavy metals in bottom sediments of the middle Odra River (Germany/Poland). Pol. J. Environ. Stud. 13 (5), 495–502.

Bower, J., Savage, K.S., Weinman, B., Barnett, M.O., Hamilton, W.P., Harper, W.F., 2008. Immobilization of mercury by pyrite (FeS2). Environ. Pollut. 156 (2), 504–514. https://doi.org/10.1016/j.envpol.2008.01.011.

Bromley, R.G., Ekdale, A.A., 1984. Chondrites: a trace fossil indicator of anoxia in sediments. Science (New York, N.Y.) 224 (4651), 872–874. https://doi.org/10.1126/science.224.4651.872.

Bryndzia, L.T., Burgess, J.M., Bourdet, J., 2023. Predicting the solubility of mercury in hydrocarbons. SPE J. 28 (02), 859–875. https://doi.org/10.2118/212271-PA.

Buatois, L.A., Mángano, M.G., 2016. Ediacaran ecosystems and the dawn of animals. In: Mángano, M.G., Buatois, L.A. (Eds.), The Trace-Fossil Record of Major Evolutionary Events: Volume 1: Precambrian and Paleozoic. Springer, Netherlands, pp. 27–72. https://doi.org/10.1007/978-94-017-9600-2_2.

Celestino, R.F.S., Ruhl, M., Dickson, A.J., Idiz, E., Jenkyns, H.C., Leng, M.J., Mattioli, E., Minisini, D., Hesselbo, S.P., 2024. Protracted carbon burial following the Early Jurassic Toarcian Oceanic Anoxic Event (Posidonia Shale, Lower Saxony Basin, Germany). Int. J. Earth Sci. 113 (8), 2023–2041. https://doi.org/10.1007/s00531-024-02477-9.

Chen, D., Ren, D., Deng, C., Tian, Z., Yin, R., 2022. Mercury loss and isotope fractionation during high-pressure and high-temperature processing of sediments: implication for the behaviors of mercury during metamorphism. Geochim. Cosmochim. Acta 334, 231–240. https://doi.org/10.1016/j.gca.2022.08.010.

Davis, R.C., Noon, S.W., Harrington, J., 2007. The petroleum potential of Tertiary coals from Western Indonesia: relationship to mire type and sequence stratigraphic setting. Int. J. Coal Geol. 70 (1), 35–52. https://doi.org/10.1016/j.coal.2006.02.008.

Dickson, A.J., Idiz, E., Porcelli, D., van den Boorn, S.H.J.M., 2020. The influence of thermal maturity on the stable isotope compositions and concentrations of molybdenum, zinc and cadmium in organic-rich marine mudrocks. Geochim. Cosmochim. Acta 287, 205–220. https://doi.org/10.1016/j.gca.2019.11.001.

Dickson, A.J., Idiz, E., Porcelli, D., Murphy, M.J., Celestino, R., Jenkyns, H.C., Poulton, S.W., Hesselbo, S.P., Hooker, J.N., Ruhl, M., van den Boorn, S.H.J.M., 2022. No effect of thermal maturity on the Mo, U, Cd, and Zn isotope compositions of Lower Jurassic organic-rich sediments. Geology 50 (5), 598–602. https://doi.org/10.1130/g49724.1.

Fabbri, D., Locatelli, C., Snape, C.E., Tarabusi, S., 2001. Sulfur speciation in mercury-contaminated sediments of a coastal lagoon: the role of elemental sulfur. J. Environ. Monit. 3 (5), 483–486. https://doi.org/10.1039/B104477J.

Fendley, I.M., Frieling, J., Mather, T.A., Ruhl, M., Hesselbo, S.P., Jenkyns, H.C., 2024. Early Jurassic large igneous province carbon emissions constrained by sedimentary mercury. Nat. Geosci. 17 (3), 241–248. https://doi.org/10.1038/s41561-024-01378-5.

Fikri, H.N., Sachsenhofer, R.F., Bechtel, A., Gross, D., 2022. Coal deposition in the Barito Basin (Southeast Borneo): the Eocene Tanjung Formation compared to the Miocene Warukin Formation. Int. J. Coal Geol. 263, 104117. https://doi.org/10.1016/j.coal.2022.104117.

Frieling, J., Fendley, I.M., Nawaz, M.A., Mather, T.A., 2024. Assessment of Hg speciation changes in the sedimentary rock record from thermal desorption characteristics. Geochem. Geophys. Geosyst. 25 ((4).). https://doi.org/10.1029/2024GC011502.

Frieling, J., Svensen, H.H., Mather, T.A., 2025. Mercury efficiently volatilized but not removed from sediments around igneous intrusions. Geology 53 (2), 176–180. https://doi.org/10.1130/G52622.1.

Frimmel, A., Oschmann, W., Schwark, L., 2004. Chemostratigraphy of the Posidonia Black Shale, SW Germany I. Influence of sea-level variation on organic facies evolution. Chem. Geol. 206 (3–4), 199–230. https://doi.org/10.1016/j.chemgeo.2003.12.007.

Ganino, C., Arndt, N.T., 2009. Climate changes caused by degassing of sediments during the emplacement of large igneous provinces. Geology 37 (4), 323–326. https://doi.org/10.1130/G25325A.1.

Goodarzi, F., Gentzis, T., Grasby, S.E., Dewing, K., 2018. Influence of igneous intrusions on thermal maturity and optical texture: comparison between a bituminous marl and a coal seam of the same maturity. Int. J. Coal Geol. 198, 183–197. https://doi.org/10.1016/j.coal.2018.09.013.

Gorbanenko, O.O., Ligouis, B., 2014. Changes in optical properties of liptinite macerals from early mature to post mature stage in Posidonia Shale (Lower Toarcian, NW Germany). Int. J. Coal Geol. 133, 47–59. https://doi.org/10.1016/j.coal.2014.09.007.

Gorbanenko, O., Ligouis, B., 2015. Variations of organo-mineral microfacies of Posidonia Shale from the Lower Saxony Basin and the West Netherlands Basin: application to paleoenvironmental reconstruction. Int. J. Coal Geol. 152, 78–99. https://doi.org/10.1016/j.coal.2015.09.011.

Grasby, S.E., Them, T.R., Chen, Z., Yin, R., Ardakani, O.H., 2019. Mercury as a proxy for volcanic emissions in the geologic record. Earth Sci. Rev. 196 (March), 102880. https://doi.org/10.1016/j.earscirev.2019.102880.

Heimdal, T.H., Svensen, Henrik, H., Ramezani, J., Iyer, K., Pereira, E., Rodrigues, R., Jones, M.T., Callegaro, S., 2018. Large-scale sill emplacement in Brazil as a trigger for the end-Triassic crisis. Sci. Rep. 8 (1), 141. https://doi.org/10.1038/s41598-017-18629-8.

Hesselbo, S., Jenkyns, H., 1995. A comparison of the Toarcian to Bajocian successions of Dorset and Yorkshire. In: Taylor, P.D. (Ed.), Field Geology of the British Jurassic. Geological Society London, pp. 105–150.

Indraswari, A.O., Frieling, J., Idiz, E., Mather, T.A., Jenkyns, H.C., Robinson, S.A., Dickson, A.J., n.d. Limited mercury (Hg) partitioning into bitumen and efficient gaseous Hg reabsorption in early thermal maturation of organic-rich mudrocks. Submitted to Geochimica et Cosmochimica Acta.

Indraswari, A.O., Frieling, J., Mather, T.A., Dickson, A.J., Jenkyns, H.C., Idiz, E., 2024. Investigating the behavior of sedimentary mercury (Hg) during burial-related thermal maturation. Geochem. Geophys. Geosyst. 25 (6). https://doi.org/10.1029/2024GC011555.

Indraswari, A.O., Frieling, J., Idiz, E., Mather, T.A., Jenkyns, H.C., Robinson, S.A., Dickson, A.J., 2025. Limited mercury (Hg) partitioning into bitumen and efficient gaseous Hg reabsorption in early thermal maturation of organic-rich mudrocks. In: Submitted to Geochimica et Cosmochimica Acta (Submitted).

Kendall, B., Wang, S., Lillis, P., Xing, L., Zheng, W., Zhu, C., 2023. Evaluation of the molybdenum isotope system as a petroleum tracer: the Phosphoria petroleum system, western U.S.A. Chem. Geol. 617, 121244. https://doi.org/10.1016/j.chemgeo.2022.121244.

Kusuma, I., Darin, T., 1989. The hydrocarbon potential of the Lower Tanjung formation, Barito Basin, S.E. Kalimantan. In: Proceedings Indonesian Petroleum Association 18th Annual Convention. IPA89-11.09, pp. 1–32.

Lang, W.D., Spath, L.F., Cox, L.R., Muir-Wood, H.M., 1928. The Belemnite Marls of Charmouth, a Series in the Lias of the Dorset Coast. Q. J. Geol. Soc. Lond. 84 (1–4), 179–222. https://doi.org/10.1144/GSL.JGS.1928.084.01-04.06.

Liu, Z., Tian, H., Yin, R., Chen, D., Gai, H., 2022. Mercury loss and isotope fractionation during thermal maturation of organic-rich mudrocks. Chem. Geol. 612 (September), 121144. https://doi.org/10.1016/j.chemgeo.2022.121144.

Lu, S.-T., Kaplan, I.R., 1989. Pyrolysis of kerogens in the absence and presence of montmorillonite—II. Aromatic hydrocarbons generated at 200 and 300°C. Org. Geochem. 14 (5), 501–510. https://doi.org/10.1016/0146-6380(89)90030-2.

O'Connor, L.K., Robinson, S.A., Naafs, B.D.A., Jenkyns, H.C., Henson, S., Clarke, M., Pancost, R.D., 2019. Late cretaceous temperature evolution of the Southern High Latitudes: a TEX86 perspective. Paleoceanogr. Paleoclimatol. 34 (4), 436–454. https://doi.org/10.1029/2018PA003546.

Patria, A.A., Suhendra, R., Anggara, F., Agangi, A., Obrochta, S.P., Setiawan, I., 2024. Association and textural-compositional evolution of pyrite-organic matter in coals of the Tarakan, Barito, and Pasir Basins, Kalimantan, Indonesia. Int. J. Coal Geol. 282, 104442. https://doi.org/10.1016/j.coal.2023.104442.

Percival, L.M.E., Bergquist, B.A., Mather, T.A., Sanei, H., 2021. Sedimentary Mercury Enrichments as a Tracer of Large Igneous Province Volcanism, pp. 247–262. https://doi.org/10.1002/9781119507444.ch11.

Ravichandran, M., 2004. Interactions between mercury and dissolved organic matter - a review. Chemosphere 55 (3), 319–331. https://doi.org/10.1016/j.chemosphere.2003.11.011.

Röhl, H.J., Schmid-Röhl, A., Oschmann, W., Frimmel, A., Schwark, L., 2001. The Posidonia Shale (Lower Toarcian) of SW-Germany: an oxygen-depleted ecosystem controlled by sea level and palaeoclimate. Palaeogeogr. Palaeoclimatol. Palaeoecol. 165 (1–2), 27–52. https://doi.org/10.1016/S0031-0182(00)00152-8.

Rumayor, M., Diaz-Somoano, M., Lopez-Anton, M.A., Martinez-Tarazona, M.R., 2015. Application of thermal desorption for the identification of mercury species in solids derived from coal utilization. Chemosphere 119, 459–465. https://doi.org/10.1016/j.chemosphere.2014.07.010.

Sanei, H., Grasby, S.E., Beauchamp, B., 2012. Latest Permian mercury anomalies. Geology 40 (1), 63–66. https://doi.org/10.1130/G32596.1.

Saniewska, D., Bełdowska, M., 2017. Mercury fractionation in soil and sediment samples using thermo-desorption method. Talanta 168, 152–161. https://doi.org/10.1016/j.talanta.2017.03.026.

Schmid-Röhl, A., Röhl, H.J., Oschmann, W., Frimmel, A., Schwark, L., 2002. Palaeoenvironmental reconstruction of Lower Toarcian epicontinental black shales (Posidonia Shale, SW Germany): global versus regional control. Geobios 35 (1), 13–20. https://doi.org/10.1016/S0016-6995(02)00005-0.

Schöllhorn, I., Adatte, T., van de Schootbrugge, B., Houben, A., Charbonnier, G., Janssen, N., Föllmi, K.B., 2020. Climate and environmental response to the break-up of Pangea during the Early Jurassic (Hettangian-Pliensbachian); the Dorset coast (UK) revisited. Glob. Planet. Chang. 185, 103096. https://doi.org/10.1016/j.gloplacha.2019.103096.

Schwark, L., Frimmel, A., 2004. Chemostratigraphy of the Posidonia Black Shale, SW-Germany II. Assessment of extent and persistence of photic-zone anoxia using aryl isoprenoid distributions. Chem. Geol. 206 (3–4), 231–248. https://doi.org/10.1016/j.chemgeo.2003.12.008.

Sellwood, B.W., 1970. The relation of trace fossils to small scale sedimentary cycles in the British Lias. In: Crimes, T.P., Harper, J.C. (Eds.), Trace Fossils. Seel House Press, pp. 489–504.

Sellwood, B.W., 1972. Regional environmental change across a Lower Jurassic stage-boundary in Britain. Palaeontology 15 (1), 125–157.

Shen, J., Algeo, T.J., Chen, J., Planavsky, N.J., Feng, Q., Yu, J., Liu, J., 2019. Mercury in marine Ordovician/Silurian boundary sections of South China is sulfide-hosted and non-volcanic in origin. Earth Planet. Sci. Lett. 511, 130–140. https://doi.org/10.1016/j.epsl.2019.01.028.

Svensen, H., Planke, S., Malthe-Sørenssen, A., Jamtveit, B., Myklebust, R., Eidem, T.R., Rey, S.S., 2004. Release of methane from a volcanic basin as a mechanism for initial Eocene global warming. Nature 429, 542–545. https://doi.org/10.1038/nature02566.

Svensen, H., Planke, S., Chevallier, L., Malthe-Sørenssen, A., Corfu, F., Jamtveit, B., 2007. Hydrothermal venting of greenhouse gases triggering Early Jurassic global warming. Earth Planet. Sci. Lett. 256 (3–4), 554–566. https://doi.org/10.1016/j.epsl.2007.02.013.

Svensen, H., Planke, S., Polozov, A.G., Schmidbauer, N., Corfu, F., Podladchikov, Y.Y., Jamtveit, B., 2009. Siberian gas venting and the end-Permian environmental crisis. Earth Planet. Sci. Lett. 277 (3), 490–500. https://doi.org/10.1016/j.epsl.2008.11.015.

Svensen, H., Fristad, K.E., Polozov, A.G., Planke, S., 2015. Volatile generation and release from continental large igneous provinces. In: Schmidt, A., Fristad, K., Elkins-Tanton, L. (Eds.), Volcanism and Global Environmental Change. Cambridge University Press, chapter, Cambridge, pp. 177–192.

Svensen, H.H., Jones, M.T., Percival, L.M.E., Grasby, S.E., Mather, T.A., 2023a. Release of mercury during contact metamorphism of shale: implications for understanding the impacts of large igneous province volcanism. Earth Planet. Sci. Lett. 619, 118306. https://doi.org/10.1016/j.epsl.2023.118306.

Svensen, H.H., Jones, M.T., Mather, T.A., 2023b. Large igneous provinces and the release of thermogenic volatiles from sedimentary basins. Elements 19 (5), 282–288. https://doi.org/10.2138/gselements.19.5.282.

Tannenbaum, E., Kaplan, I.R., 1985. Role of minerals in the thermal alteration of organic matter—I: generation of gases and condensates under dry condition. Geochim. Cosmochim. Acta 49 (12), 2589–2604. https://doi.org/10.1016/0016-7037(85)90128-0.

Tissot, B.P., Welte, D.H., 1984. Petroleum Formation and Occurrence. In: Petroleum formation and occurrence, 2nd rev. a. Springer-Verlag. https://doi.org/10.1007/978-3-642-96446-6_5.

Wallschläger, D., Desai, M.V.M., Spengler, M., Wilken, R.-D., 1998. Mercury speciation in floodplain soils and sediments along a contaminated river transect. J. Environ. Qual. 27, 1034–1044. https://doi.org/10.2134/jeq1998.00472425002700050008x.

Weedon, G.P., Jenkyns, H.C., 1990. Regular and irregular climatic cycles and the Belemnite Marls (Pliensbachian, Lower Jurassic, Wessex Basin). J. Geol. Soc. Lond. 147 (6), 915–918. https://doi.org/10.1144/gsjgs.147.6.0915.

Weedon, G.P., Jenkyns, H.C., 1999. Cyclostratigraphy and the Early Jurassic timescale: data from the Belemnite Marls, Dorset, southern England. GSA Bull. 111 (12), 1823–1840. https://doi.org/10.1130/0016-7606(1999)111<1823:CATEJT>2.3.CO;2.

Witts, D., Hall, R., Nichols, G., Morley, R., 2012. A new depositional and provenance model for the Tanjung Formation, Barito Basin, SE Kalimantan, Indonesia. J. Asian Earth Sci. 56, 77–104. https://doi.org/10.1016/j.jseaes.2012.04.022.

Xu, J., Bland, G.D., Gu, Y., Ziaei, H., Xiao, X., Deonarine, A., Reible, D., Bireta, P., Hoelen, T.P., Lowry, G., v., 2021. Impacts of sediment particle grain size and mercury speciation on mercury bioavailability potential. Environ. Sci. Technol. 55 (18), 12393–12402. https://doi.org/10.1021/acs.est.1c03572.